Nano LIFE
(2026) 2550009 (10 pages)

DOI: 10.1142/S1793984425500096

World Scientific
www.worldscientific.com

On the Local Nanoscale Temperature Distributions in Photothermal Systems

Donglu Shi
Materials Science and Engineering
College of Engineering and Applied Science
University of Cincinnati
Cincinnati, OH 45221, USA
donglu.shi@uc.edu

Received 27 June 2025
Accepted 30 July 2025
Published 28 August 2025

Accurate temperature measurement at the nanoscale is essential for a wide range of applications in nanomedicine, energy conversion, and materials science. In this study, we present a theoretical framework to determine the minimum number of nanoparticles required to obtain statistically meaningful temperature readings based on thermal fluctuations and ensemble averaging. Using principles from statistical mechanics and thermodynamics, we derive criteria that link nanoparticle count, measurement variance, and thermal resolution. We further raise a fundamental but largely overlooked question: *Can a well-defined temperature profile exist at the nanoscale, and if so, what are its spatial boundaries*? This work provides a conceptual and statistical foundation for understanding nanoscale temperature distributions in photothermal systems, with thermodynamic implications for diagnostics, thermal therapy, and nanoscale energy applications.

Keywords: Nanoparticles; nanoscale temperature; photothermal therapy; nanomedicine; cancer treatment; temperature profiling; statistical modeling; localized surface plasmon resonance (LSPR); thermal dynamics.

1. Introduction

In nanomedicine, plasmonic nanoparticles have been widely applied in medical diagnosis and therapeutics, especially in photothermal therapy (PTT).[1–8] In PTT, the Fe_3O_4 nanoparticles are dispersed in solutions and mixed with cells for *in vitro* experiments or IV-injected into the bloodstream through the tail vein for *in vivo* studies. In a typical *in vitro* experiment, the surface-functionalized Fe_3O_4 magnetic nanocomposites (MNCs) can bind onto the cell surfaces intimately via various cell targeting means as shown in Fig. 1(a).[1] As shown in Fig. 1(a), the MNCs are labeled with fluorescein isothiocyanate (FITC), which produces green fluorescence, while the nuclei of HeLa cells are stained blue with DAPI. Due to the negative surface charge of the cancer cells, the positively charged MNCs bind closely and selectively to the cell membranes. Upon laser irradiation (typically 808 nm), the Fe_3O_4 MNCs can generate sufficient heat via the so-called Localized Surface Plasmon

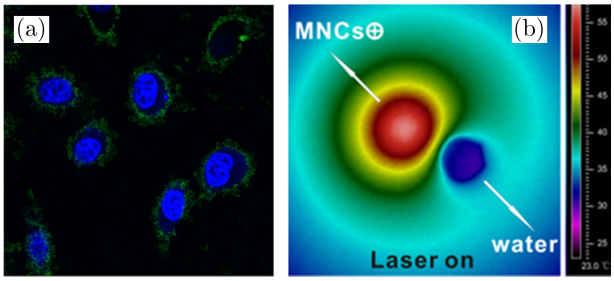

Fig. 1. (a) Fluorescence confocal images of HeLa cells with Fe_3O_4 nanoparticles surrounding them. The surface-functionalized Fe_3O_4 MNCs are labeled with FITC (green) while DAPI is used to stain the cell nucleus (blue). (b) The NIR thermal images of a droplet of PBS solution with MNCs and a droplet of PBS blank on the glass slide (color online).[1]

Resonance (LSPR),[9,10] raising the environmental temperature to 42–45°C [Fig. 1(b)], leading to thermal ablation of cancer cells.[1] The ability to measure the local temperature at the interfaces between the biological cells and nanoparticles is critical for optimizing therapy and ensuring that the heat dose is sufficient to cause cellular damage without affecting surrounding healthy tissue. The thermal image of a PBS droplet containing MNCs clearly demonstrates this localized heat generation [Fig. 1(b)], in contrast to the nonheated PBS control, thereby providing visual evidence of nanoparticle-mediated photothermal response. This localized heating can lead to thermal ablation of cancer cells while minimizing damage to the surrounding healthy tissue. Critically, the ability to measure and model local temperatures at the nanobio interface is essential for optimizing treatment parameters and ensuring therapeutic efficacy with spatial precision.

While an isolated nanoparticle lacks a thermodynamic temperature in the classical sense due to large energy fluctuations, real-world systems are rarely isolated. In biological environments, nanoparticles interact continuously with their surroundings — such as solvent molecules and cellular membranes — which serve as thermal reservoirs. These interactions mediate energy exchange and vibrational equilibration, allowing an effective temperature to be defined via coupling with the bath. Our statistical treatment focuses on estimating the lower bounds for meaningful temperature definitions, which remain relevant even under partial thermal coupling conditions. Future models will incorporate environment-mediated damping and stochastic heat exchange for a more complete picture.

The interaction of Fe_3O_4 nanoparticles with biological cells occurs at the nanometer scale, where heat dissipation is highly localized, especially at the very initial stage of laser irradiation in PTT. The nanobio interface behavior is critical in the understanding of the biological and therapeutic mechanisms. The common procedure of determining the therapeutic efficacy mainly relies on the cell viability profiles against nanoparticle concentration and environmental temperature, which are statistically averaged without any nanoscale behavior observations. More importantly, the temperature profiles are averaged over the entire system without any microscopic temperature analysis in both *in vitro* and *in vivo* experiments. Studying the nanoscale behavior at the cellular level remains a significant challenge, especially when only a few nanoparticles are present on the cell surface. The key is to be able to establish a local temperature profile within the vicinity of a nanoparticle across the cell membrane for observation of the local and interfacial behaviors in a temporal and spatial manner.

Conventional temperature measurement techniques, such as thermocouples or infrared thermometry, lack the spatial resolution necessary to accurately determine the temperature at the interfaces between nanoparticles and biological cells/tissues at the nanoscale. More fundamentally, temperature is a statistical property emerging from the collective motion of many particles[11–13]; an isolated Fe_3O_4 nanoparticle does not possess a well-defined temperature. Therefore, the key question is whether *a well-defined temperature profile exists at the nanoscale, and if so, what are its spatial boundaries*? Is it possible to establish a critical number of particles (or cluster size) for meaningful temperature at nanoscale? Below this threshold, thermal fluctuations become dominant, and classical thermodynamic concepts break down.

This study provides a statistical approach to determine the critical number of nanoparticles (or critical cluster size) necessary for a reliable temperature measurement under photothermal heating. This study aims to bridge the gap between nanoscale heat generation and macroscopic temperature measurements. The results of this study can provide insights into how to optimize nanoparticle concentration, laser parameters, and treatment conditions for effective cancer therapy.

2. Results

2.1. *Statistical analysis of temperature*

We first determine the number of particles required to generate a statistically meaningful local temperature profile at the nanoscale. For a solid nanoparticle system in thermal equilibrium, each atom vibrates about its equilibrium position and the total internal energy includes both kinetic and potential energy contributions from vibrational modes. According to the equipartition theorem in the classical limit, each vibrational degree of freedom contributes $(½)k_BT$ of kinetic energy and $(½)k_BT$ of potential energy. In three dimensions, each atom has three vibrational modes, totaling six degrees of freedom, which yields a mean total energy per particle of:

$$\langle E \rangle = 3k_BT, \tag{1}$$

where k_B is the Boltzmann constant and T is the absolute temperature. This internal energy sets the scale for thermally driven processes and fluctuations within the nanoparticle. The total energy of the system depends on the number of constituent particles and governs the statistical precision of local temperature measurements. The number of particles must be sufficiently large such that statistical fluctuations in energy are small compared with the average energy, thereby ensuring that the concept of temperature is well-defined at the nanoscale.

In a solid nanoparticle system, each atom vibrates about its equilibrium position, and the internal energy comprises both kinetic and potential components arising from these vibrations. According to the equipartition theorem in the classical limit, each vibrational degree of freedom contributes $(½)k_BT$ of potential energy. Since each atom in three dimensions has three vibrational modes (totaling six degrees of freedom), the average total internal energy of the system is[11–13]:

$$\langle E_{\text{total}} \rangle = 3Nk_BT, \tag{2}$$

where N is the number of atoms and T is the absolute temperature. This internal energy governs the thermal behavior and fluctuation statistics of the system. We adopt this total energy as the basis for subsequent analysis of temperature fluctuation and statistical convergence.

To achieve a desired precision ΔT in the temperature, the number of particles must satisfy:

$$N \geq \left(\frac{T}{\Delta T} \right)^2. \tag{3}$$

For example, achieving 1% precision in temperature (i.e., $\Delta T/T = 0.01$) requires:

$$N \geq \left(\frac{1}{0.01} \right)^2 = 10^4. \tag{4}$$

This condition ensures that the statistical temperature measurement is meaningful. In the case of Fe_3O_4 nanoparticles, even a small number of atoms (on the order of 10^4) can suffice to define a temperature profile with adequate precision for localized photothermal heating, particularly in biomedical applications like cancer therapy.

For 0.1% precision, this requirement increases to: $N \geq 10^6$.

It is important to note that the above statistical considerations apply to a thermodynamic system characterized by effective thermal interactions among its constituents. In the context of nanoparticles, this implies that the particles must be sufficiently close or clustered such that energy exchange between them occurs on timescales relevant to thermal equilibration. Such interaction can occur via direct physical contact, near-field thermal radiation, or conduction through the surrounding medium. This interaction justifies treating the collection of nanoparticles as a unified system, allowing the constituent atoms across different particles to be collectively considered in the statistical energy fluctuation analysis. Consequently, the derived particle number thresholds represent the minimum cluster size required to establish a well-defined local temperature rather than the count of isolated, thermally independent nanoparticles.

2.2. *Number of atoms per nanoparticle*

Let's calculate how many atoms are there in one 10-nm Fe_3O_4 nanoparticle.

Volume of a nanoparticle (sphere):

$$V = \frac{4}{3}\pi r^3 = \frac{4}{3}\pi \left(5 \times 10^{-9}\,\text{m}\right)^3 = 5.24 \times 10^{-25}\,\text{m}^3 \tag{5}$$

Density of Fe_3O_4:

$$\rho = 5.2\ g/\text{cm}^3 = 5200\ kg/\text{m}^3$$

Mass of one nanoparticle:

$$m = \rho \cdot V = 5200 \times 5.24 \times 10^{-25} = 2.72 \times 10^{-21}\ \text{kg}. \quad (6)$$

Molar mass of Fe_3O_4:

$$M = 231.5\ g/\text{mol} = 0.2315\ \text{kg/mol}$$

Number of atoms per nanoparticle:

$$n = \frac{M}{m} \times N_A = \frac{0.2315}{2.72 \times 10^{-21}} \times 6.022 \times 10^{23} \approx 4.27 \times 10^3\ \text{atoms}$$

So, each 10 nm Fe_3O_4 nanoparticle contains roughly 4270 atoms.

2.3. *Number of nanoparticles required*

To have: $\geq 10^4$ atoms (1% energy fluctuation):

$$\frac{4.27 \times 10^3\ \text{atoms/NP}}{10^4\ \text{atoms}} \approx 2.34 \Rightarrow \text{At least 3 nanoparticles}$$

$\geq 10^4$ atoms (0.1% energy fluctuation):

$$\frac{4.27 \times 10^3}{10^6} \approx 234 \Rightarrow \text{At least 234 nanoparticles}$$

2.4. *Spatial scale of such a cluster*

Assuming nanoparticles are packed densely:

$$V_{\text{cluster}} = 234 \times 5.24 \times 10^{-25} \approx 1.23 \times 10^{-22}\ \text{m}^3. \quad (7)$$

Thus, to establish a local temperature with 0.1% precision, a cluster of ≥ 234 Fe_3O_4 nanoparticles is needed, corresponding to a spatial extent of approximately 50 nm. For 1% precision, only three nanoparticles can establish the local temperature profile with a spatial scale of 20 nm (Table 1).

Table 1 Number of nanoparticles required for local temperature established and related special scale for 0.1% and 1.0% precision, respectively.

Requirement	# Atoms needed	# NPs needed	Spatial scale
1.0% precision	10^4	~3	~20 nm
0.1% precision	10^6	~234	~50 nm

This provides a lower bound on the spatial scale at which a well-defined local temperature can be assumed for nanoscale thermal analysis.

If we consider 1% precision, only a few nanoparticles are required for establishing the local temperature profile with a spatial scale of 20 nm. Figure 2 schematically illustrates the local temperature profile on a cell surface with a few nanoparticles. As shown in this figure, the nanoparticles on the cell membrane surface may not be evenly distributed. At a location with a nanoparticle cluster (~50 nm), the temperature variation occurs as depicted in this figure.

In a previous study,[1] we conducted photothermal experiments with surface-functionalized Fe_3O_4 MNCs of various concentrations dispersed in PBS. As shown in Fig. 3, upon irradiation with a 808 nm laser (2W/cm^2), with a concentration of 0.15 mg/mL MNCs, the solution temperature reaches ~ 50°C from an initial 25°C within 2 min ($\Delta T = 50°C - 25°C = 25°C$).[1] Expectedly, the local cell surface temperature would initially be higher than the average solution temperature since the MNCs are the original heat source, which are directly irradiated with an 808 nm laser. The local nanoparticle temperature responds to laser irradiation much faster, starting at ~80°C and decaying exponentially toward the bulk temperature due to heat diffusion into the surrounding fluid.

In general, under laser irradiation, the nanoparticles absorb NIR light and rapidly convert it to

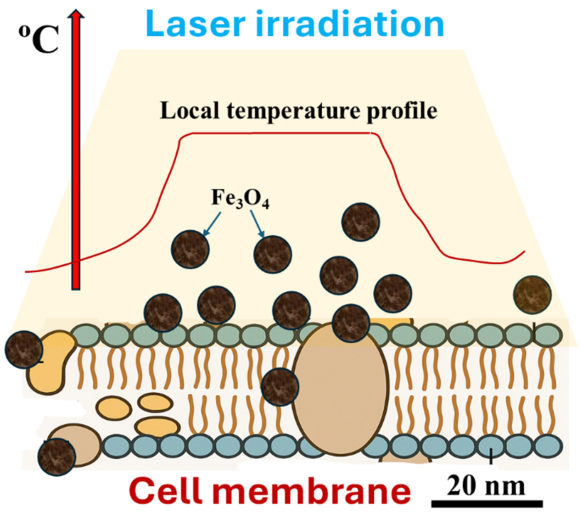

Fig. 2. Schematic diagram illustrates the local temperature profile over a small cluster of nanoparticles (~50 nm) on the surface of the cell membrane.

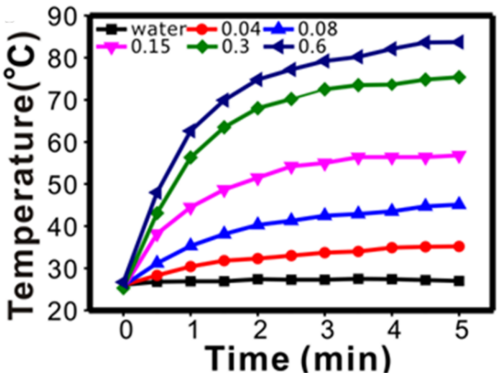

Fig. 3. Photothermal heating curves of surface-functionalized Fe_3O_4 MNCs under 808 nm laser ($2W/cm^2$) of various concentrations as indicated (mg/mL). For the concentration of 0.15 mg/mL (pink curve), the temperature reaches ~50°C at 2 min (color online).[1]

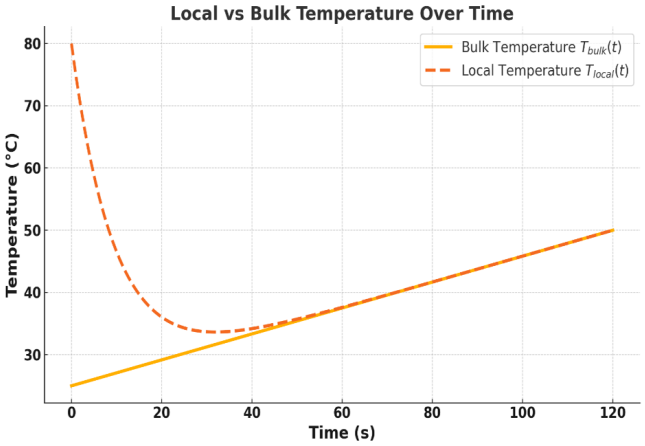

Fig. 4. Local temperature evolution $T_{\text{local}}(t)$, of nanoparticles relaxing toward a linearly increasing bulk temperature $T_{\text{bulk}}(t)$ from 25°C to 50°C. The initial local temperature is set at 80°C, and the thermal relaxation time is $\tau = 10$ s. While this plot illustrates the temporal response of nanoscale thermal environments, it is only physically meaningful when the concept of local temperature is statistically justified. This statistical threshold sets the lower bound on spatial resolution for meaningful nanoscale temperature analysis.

thermal energy via nonradiative relaxation of excited electrons via the following mechanisms: (1) The nanoparticle is the direct absorber of light; (2) it is much smaller than the surrounding thermal diffusion length, and (3) the heat is initially confined to the immediate vicinity of the nanoparticle. This means that before heat has time to dissipate into the surrounding medium, the temperature right at or near the nanoparticle surface can rise significantly higher than the average solution temperature. Previous studies[14–16] have demonstrated that a 10–100 nm metallic nanoparticle under laser intensities of 1–2 W/cm^2 can easily reach surface temperatures of 70–90°C within milliseconds. The local temperature differences between the nanoparticle and the bulk are commonly reported in the first few seconds of irradiation. For Fe_3O_4, which is less optically absorbing than gold but still effective under NIR, a conservative estimate of ~80°C local temperature is reasonable with 2 W/cm^2 irradiation, assuming efficient clustering on cell surfaces.

The resulting plot of temperature versus time from Eq. (8) is shown in Fig. 4. As shown in this figure, the local temperature near the nanoparticle surface can significantly exceed the bulk solution temperature due to the nanoscale confinement of absorbed energy. Unlike bulk solution, photothermal conversion in nanoparticles involves the absorption of photons by electrons and their subsequent nonradiative relaxation into lattice vibrations (phonons), rapidly generating localized heat. In our system, while the average bulk solution temperature rises from 25°C to ~50°C within 120 s, we estimate that the local temperature at nanoparticle-rich regions may initially reach up to ~80°C before thermal diffusion equilibrates the system. This transient temperature elevation is particularly important for applications such as photothermal therapy, where localized heating can induce cellular effects well before the surrounding medium reaches uniform temperature.

We assume an exponential decay governed by

$$T_{\text{local}}(t) = T_{\text{bulk}}(t) + \left(T_{\text{initial}} - T_{\text{bulk}}(t)\right) \cdot e^{-t/\tau}, \quad (8)$$

where

$T_{\text{initial}} = 80°C$

$T_{\text{bulk}}(t)$ rises linearly from 25°C to 50°C at 2 min

$\tau = 10$ s (typical thermal relaxation time at nanoscale)

Upon laser irradiation, Fe_3O_4 nanoparticles absorb near-infrared (NIR) photons primarily through electronic excitation. This energy is initially deposited into the electronic subsystem, generating a population of nonequilibrium "hot" electrons.[17,18] Within tens to hundreds of femtoseconds, electron–electron scattering redistributes this energy, establishing a quasi-equilibrium Fermi–Dirac distribution characterized by an elevated electron temperature (T_e). Subsequently, over a few picoseconds, energy is transferred from the hot electrons to the atomic lattice via

electron–phonon coupling, raising the lattice temperature (T_{lattice}) and initiating phonon-mediated heat generation. This thermal energy then diffuses into the surrounding medium (e.g., aqueous environment or biological cell), leading to measurable heating effects.

Although the photothermal process is initiated by electrons, the physically relevant and sustained temperature rise corresponds to the lattice temperature, as it governs atomic vibrations and thermal energy exchange with the environment. Therefore, temperature in the context of nanoparticle-mediated heating is defined by the vibrational energy of atoms rather than electronic excitation alone. This justifies the use of atomic count to establish the statistical precision of temperature measurement. For instance, to achieve 1% precision in defining a local temperature field, the system must contain at least atoms, a condition readily satisfied even by single nanoparticles in the 10–50 nm size range. This thermodynamic definition aligns with macroscopic temperature concepts and underpins the meaningful interpretation of localized heating effects in biomedical and energy applications.

The total vibrational energy E_{vib} of a crystalline lattice at temperature T is given by summing the energy over all phonon modes:

$$E_{\text{vib}} = \sum_{\vec{q},s} \hbar\omega_{\vec{q},s}\left(n_{\vec{q},s} + \frac{1}{2}\right), \tag{9}$$

where
- $\vec{q}$: Phonon wavevector
- s: Phonon branch (acoustic or optical)
- $\omega_{\vec{q},s}$: Phonon frequency of mode $(\vec{q},s)$
- $\hbar$: Reduced Planck constant
- $n_{q,s}$: Occupation number given by the Bose–Einstein distribution:

$$n_{\vec{q},s} = \frac{1}{\exp\left(\frac{\hbar\omega_{\vec{q},s}}{k_B T}\right) - 1}. \tag{10}$$

The zero-point energy $(1/2)\hbar\omega_{\vec{q},s}$ represents the vibrational energy at 0 K and is often subtracted in thermal calculations.

To estimate the total lattice vibrational energy in solids like Fe_3O_4 nanoparticles, the Debye model provides a useful approximation:

$$E_{\text{vib}} = 9Nk_B T\left(\frac{\Theta_D}{T}\right)^3 \int_0^{\frac{\Theta_D}{T}} \frac{e^x}{\left(e^x - 1\right)} x^3\, dx, \tag{11}$$

where
- N: Total number of atoms in the system
- k_B: Boltzmann constant
- Θ_D: Debye temperature of the material
- $x = \hbar\omega/k_B T$: Dimensionless variable

At temperatures much higher than the Debye temperature ($T \gg \Theta_D$), the integral converges and the vibrational energy simplifies to

$$E_{\text{vib}} \approx 3Nk_B T. \tag{12}$$

This expression corresponds to the classical limit of the equipartition theorem, where each of the 3N phonon modes contributes energy $k_B T$.

For 234 Fe_3O_4 nanoparticles (10 nm diameter) containing approximately $N = 10^6$ atoms in total, and assuming room-to-moderate heating (~323 K), the lattice vibration energy can be approximated using the high-temperature limit:

$$E_{\text{vib}} \approx 3 \times 10^6 \times \left(1.38 \times 10^{-23}\right) \times 323 \approx 1.34 \times 10^{-14}\ J$$

This quantifies the thermal energy stored in phonon modes and helps describe the thermodynamically defined temperature increase in nanoparticle photothermal heating.

To estimate the instantaneous temperature rise of 234 Fe_3O_4 nanoparticles (~10^6 atoms total) under 808 nm laser irradiation at 2 W/cm^3 for 2 min, before heat is lost to the environment, we can use the basic energy balance:

Laser power density: $P = 2\ \text{W/cm}^3 = 2 \times 10^6\ \text{W/m}^3$

Irradiation time: $t = 120\ \text{s}$

Absorption efficiency (η): assume 100% (upper limit, no losses)

Volume occupied by particles: assume they are suspended in a very small volume

$V \approx 10^{-12}\ \text{m}^3$(1 nanoliter) or smaller (see below)

Specific heat capacity of Fe_3O_4 nanoparticles: $V \approx 10^{-12}\ \text{m}^3$

Density of Fe_3O_4: $\rho \approx 5.17 \times 10^3\ \text{kg/m}^3$

$$Q = P \cdot V \cdot t = (2\times10^{6})\,W/m^{3} \cdot V \cdot 120\,s = 2.4\times10^{8} \cdot VJ$$

$$Q = mC_{p}\Delta T$$

$$\text{where} \quad m = \rho \cdot V \quad \Rightarrow \quad \Delta T = \frac{Q}{mC_{p}} = \frac{\rho V C_{p}}{2.4\times10^{8}}$$

$$\Delta T = \frac{\left(5.17\times10^{3}\right)\cdot(670)}{2.4\times10^{8}} = \frac{3.47\times10^{6}}{2.4\times10^{8}} \approx 69.2\,K$$

The temperature rise is approximately 69°C, assuming:

all laser energy is absorbed (100% efficiency),

no heat loss to the environment during the 2 min exposure,

particles are in a very small, confined volume where laser intensity is effectively delivered.

Thus, if the initial temperature is 25°C, the nanoparticles could momentarily reach:

$$T_{\text{final}} \approx 25°\text{C} + 69°\text{C} = 94°\text{C}$$

The analytically estimated temperature rise resulting from laser irradiation (2 W/cm^2 for 2 min) yields a final temperature of approximately 94°C under idealized full absorption conditions. This result is in strong agreement with prior experimental observations, which report nanoparticle surface temperatures in the range of 70–90°C for similar laser intensities and particle sizes.[14–16] The working assumption of 80°C in our model thus represents a physically reasonable estimate, accounting for partial absorption and realistic photothermal conversion efficiencies in the range of 85–90%. This consistency between the calculated thermal energy deposition, vibrational energy distribution among lattice phonons, and empirically observed temperatures validates our approach and reinforces the thermodynamic relevance of lattice vibrations in defining the local temperature field of laser-heated nanoparticles.

It must be noted that Fig. 4 is only valid if the local temperature can be established at the nanoscale, as depicted in Fig. 2. Otherwise, the statistical characteristics of temperature may not be meaningful in a nanoscale cluster of nanoparticles. The plot of the local temperature $T_{\text{local}}(t)$, which relaxes toward the linearly increasing bulk temperature $T_{\text{bulk}}(t)$ over time, illustrates the thermal response of nanoparticles in a dynamic environment. However, this plot alone is not physically meaningful unless the statistical foundation for defining a local temperature is established. A well-defined local temperature at the nanoscale requires a minimum number of particles to ensure statistical significance. Specifically, achieving 0.1% temperature precision demands a cluster of at least 234 Fe_3O_4 nanoparticles (~50 nm spatial extent), while 1% precision requires only about three nanoparticles (~20 nm scale). Thus, this statistical threshold provides the necessary justification for interpreting the local temperature behavior shown in the plot.

It should be noted that nanoparticles may aggregate or adhere unevenly to cell surfaces. Such nonuniform distributions can result in localized temperature hotspots or thermal gradients that deviate significantly from the predictions of the idealized model. Clustering of nanoparticles can enhance localized photothermal conversion, leading to nonlinear thermal responses that complicate both measurement accuracy and therapeutic control in applications such as photothermal therapy (PTT). Incorporating spatial heterogeneity and aggregation effects into future models — possibly through Monte Carlo simulations or spatial heat transport equations —will improve predictive accuracy and help refine nanoparticle dosing strategies. Experimental validation using high-resolution thermal imaging could further elucidate the impact of nonuniform nanoparticle distribution.

3. Discussion

This work serves as an initial communication to highlight a critical yet often overlooked issue in nanoscale thermal analysis: the statistical and spatial boundaries necessary for defining a meaningful temperature near the nanobio interface. While our current treatment employs classical statistical thermodynamics to estimate the critical number of nanoparticles required for stable local temperature profiles, a comprehensive understanding of temperature at the nanoscale must integrate frameworks from nonequilibrium and stochastic thermodynamics. In rapidly evolving systems under laser irradiation — where energy input and dissipation are inherently dynamic — the conventional concept of equilibrium temperature becomes inadequate. Future research should

explore effective temperatures derived from fluctuation–dissipation relations, entropy production, and other nonequilibrium constructs. Additionally, theoretical principles such as the Landauer limit, which links information processing with thermal energy dissipation, may shed light on fundamental constraints of thermal definition and control at the nanoscale. These advanced frameworks, alongside molecular dynamics or Monte Carlo simulations, will be crucial for refining the current model and enabling predictive, mechanism-based design of photothermal therapies.

Although the use of statistical fluctuations to estimate temperature stability is standard in thermodynamics, its application in nanoscale photothermal contexts is both relevant and nontrivial. Particularly, in biomedical environments where only a small number of nanoparticles interact with cells, it is essential to establish quantitative spatial bounds within which the concept of temperature remains valid. Our approach provides a straightforward yet powerful estimate of the minimum nanoparticle cluster size needed to define a local temperature with statistical significance, offering practical implications for photothermal therapy design, where spatial precision and heat dose control are paramount. Nonetheless, this model represents a first-order approximation. Future work should include higher-order effects such as energy distribution variance, finite-size heat capacity anomalies, and quantum confinement phenomena, which can significantly influence thermal behavior at the nanoscale. Incorporating these factors would refine the spatial resolution limits of temperature definition and yield more accurate predictions for practical applications.

In systems subjected to rapid energy input, like laser-irradiated nanoparticle clusters, the assumption of local thermal equilibrium breaks down, making the definition of conventional temperature problematic. Alternative concepts, such as effective temperature, become necessary. One formalism for effective temperature is based on the fluctuation–dissipation theorem (FDT), which in equilibrium relates a system's response to perturbations with fluctuations in observables. Out of equilibrium, this relation is violated. Cugliandolo and Kurchan[19] introduced a generalized fluctuation–dissipation ratio interpretable as an effective temperature, especially in systems with slow relaxation dynamics such as glasses or driven nanoscale assemblies. Similarly, the Hatano–Sasa relation[20] offers a framework for entropy production and thermodynamics in driven nonequilibrium systems, providing further insight into how effective temperatures arise from stochastic dynamics.

While the above treatment (Eqs. (1)–(4)) holds under equilibrium conditions, laser-induced photothermal heating drives the system far from equilibrium. In such scenarios, the concept of a single, well-defined temperature becomes nontrivial. In equilibrium, the FDT links the response function $R(t)$ of a system to its spontaneous fluctuations $C(t)$:

$$R(t) = -\frac{1}{k_B T}\frac{dC(t)}{dt}. \tag{13}$$

Under nonequilibrium conditions (e.g., pulsed laser excitation), this relationship breaks down. The deviation from FDT allows for the definition of an effective temperature T_{eff}:

$$T_{\text{eff}} = -\frac{1}{k_B}\left(\frac{dC(t)}{dt}/R(t)\right). \tag{14}$$

This dynamic, time-dependent temperature governs how energy is dissipated and redistributed in driven nanosystems and may differ substantially from the bath temperature or kinetic definitions.

In systems with persistent energy input, such as PTT-driven nanoparticle clusters, temperature becomes trajectory-dependent. The Cugliandolo–Kurchan framework introduces T_{eff} as a slow-mode descriptor in systems with aging or glassy dynamics, while the Hatano–Sasa identity generalizes fluctuation theorems to steady-state driven systems, enabling formal definitions of entropy production and thermodynamic observables without detailed balance. These models suggest that local temperatures near a nanoparticle surface may vary both spatially and temporally, governed by energy dissipation pathways, particle–matrix coupling, and nonequilibrium fluctuations.

At low N, classical assumptions about energy distributions also break down. While energy fluctuations in large systems obey a Gaussian distribution (from the Central Limit Theorem), in small clusters or transient states, distributions may become skewed, non-Gaussian, or follow exponential tails. This shift reflects the non-Boltzmann nature of particle energy states in nanoscale environments.

Thus, the assumption that $\langle E_k \rangle \propto T$ must be carefully revisited when designing or interpreting nanoscale thermometric systems under dynamic thermal fields. Recognizing and modeling these nonequilibrium behaviors is essential to developing accurate temperature probes and optimizing photothermal therapies at the nanoscale.

A natural extension of this work would involve Monte Carlo (MC) or molecular dynamics (MD) simulations to model nanoparticle clusters under photothermal heating and extract spatial and temporal temperature fluctuations. Such simulations would better capture interparticle interactions, heat conduction to the environment, and nonequilibrium effects including transient hot spots and thermal gradients near the nanobio interface. Although beyond the scope of this initial communication, these simulations represent a critical next step for validating the statistical thresholds derived here and refining the nanoscale temperature concept. Previous MD studies have revealed significant nonequilibrium thermal phenomena in metallic and magnetic nanoparticles under laser excitation,[21–23] including localized heating, transient temperature gradients, and departures from bulk thermal conductivity. Coupling our analytical framework with these computational approaches could bridge the gap between theory and realistic dynamic behavior, enabling predictive design of nanoparticle clusters for efficient and spatially controlled photothermal therapy.

4. Conclusion

In this brief report, we aimed to highlight a key conceptual issue that has not received sufficient attention: the feasibility and definition of a temperature profile at the nanoscale. Our analysis was intentionally focused and limited in scope, serving as a preliminary step toward more detailed experimental investigations and assessments of biological implications, which are subjects of future research. This study establishes a quantitative statistical framework for determining the minimum number of nanoparticles required to achieve reliable and meaningful temperature measurements at the nanoscale. By linking thermal energy fluctuations with ensemble averaging, we provide a model that predicts how nanoparticle count directly affects the accuracy of temperature readings. Our results highlight that as the number of sensing nanoparticles increases, the thermal noise decreases proportionally, enabling more precise temperature detection. Importantly, this theoretical foundation offers practical guidance for experimental design in nanoscale thermal sensing, ensuring that measurement uncertainty can be minimized through proper nanoparticle selection and deployment. The outcome of this research provides a critical correlation between statistical thermodynamic theory and experimental implementation, paving the way for more accurate, scalable, and application — specific thermal sensors in fields ranging from nanomedicine to energy materials.

Conflict of Interest

Donglu Shi declares that, as Editor-in-Chief of this journal, there is a conflict of interest regarding this paper. However, Donglu Shi confirms that he was not involved in the peer review procedure of this paper, which was handled by an Associate Editor of the journal, and therefore, he did not influence the editorial decision-making process. The conflict of interest was disclosed to the editorial team, and appropriate steps were taken to ensure that the peer review and decision-making process for this paper were handled impartially and transparently.

Statement of Usage of Artificial Intelligence

Figures 2 and 4 were plotted using AI-assisted tools.

Data Availability Statement

The data supporting the findings of this study are available from the corresponding author upon reasonable request.

Funding Information

We gratefully acknowledge the financial support provided by the National Science Foundation (Grant No. CMMI-1953009).

ORCID

Donglu Shi
https://orcid.org/0000-0002-0837-7780

References

1. X. Han, Z. Deng, Z. Yang, Y. Wang, H. Zhu, B. Chen, Z. Cui, R. C. Ewing and D. Shi, *Nanoscale* **9**, 1457 (2017).
2. A. W. Dunn, Y. Zhang, D. Mast, G. M. Pauletti, H. Xu, J. Zhang, R. C. Ewing and D. Shi, *Mater. Sci. Eng. C* **69**, 12 (2016).
3. A. W. Dunn, S. M. Ehsan, D. Mast, G. M. Pauletti, H. Xu, J. Zhang, R. C. Ewing and D. Shi, *Mater. Sci. Eng. C* **46**, 97 (2015).
4. M. Chu, H. Li, Q. Wu, F. Wo and D. Shi, *Biomaterials* **35**, 8357 (2014).
5. M. Chu, Y. Shao, J. Peng, X. Dai, H. Li, Q. Wu and D. Shi, *Biomaterials* **34**, 4078 (2013).
6. X. Zhang, Y. Liu, S. T. Lee, S. Yang and Z. Kang, *Nanomedicine* **10**, 527 (2014).
7. W. C. Chan and S. Nie, *Science* **281**, 2016 (1998).
8. C. Kong and X. Chen, *Int. J. Nanomedicine* **17**, 6427 (2022), doi: 10.2147/IJN.S388996.
9. M. Shabaninezhad and G. Ramakrishna, *J. Chem. Phys.* **150**, 144116 (2019).
10. A. Agrawal, S. H. Cho, O. Zandi, S. Ghosh, R. W. Johns and D. J. Milliron, *Chem. Rev.* **118**, 3121 (2018), doi: 10.1021/acs.chemrev.7b00613.
11. F. Reif, *Fundamentals of Statistical and Thermal Physics* (McGraw-Hill, New York, 1965).
12. G. H. Wannier, *Statistical Physics* (Dover Publications, New York, 1987).
13. F. Mandl, *Statistical Physics* (Wiley, New York, 1988).
14. G. Baffou and R. Quidant, *Laser Photon. Rev.* **7**, 171 (2013).
15. G. Baffou and R. Quidant, *ACS Nano* **7**, 1558 (2013).
16. S. J. Oldenburg, R. D. Averitt, S. L. Westcott and N. J. Halas, *Chem. Phys. Lett.* **288**, 243 (1998).
17. M. Kim, J.-H. Lee and J.-M. Nam, *Adv. Sci.* **6**, 1900471 (2019), https://doi.org/10.1002/advs.201900471.
18. H. P. Paudel, A. Safaei and M. N. Leuenberger, Nanoplasmonics in metallic nanostructures and Dirac systems, in *Nanoplasmonics — Fundamentals and Applications*, ed. G. Barbillon (InTech, 2017), pp. 1–28, doi: 10.5772/67689.
19. L. F. Cugliandolo and J. Kurchan, *Phys. Rev. Lett.* **71**, 173 (1993).
20. T. Hatano and S.-I. Sasa, *Phys. Rev. Lett.* **86**, 3463 (2001).
21. T. S. van Erp, S. Curat and M. Mareschal, *Phys. Rev. B* **87**, 195418 (2013).
22. G. Baffou and R. Quidant, *Laser Photonics Rev.* **7**, 171 (2013).
23. P. Keblinski, D. G. Cahill, A. Bodapati, C. R. Sullivan and T. A. Taton, *J. Appl. Phys.* **100**, 054305 (2006).